Inorg. Chem. **2003**, *42*, 4117–4126

Solution Behavior and Structural Diversity of Bis(dialkylphosphino)methane Complexes of Palladium

Craig B. Pamplin, Steven J. Rettig,† Brian O. Patrick, and Brian R. James*

Department of Chemistry, University of British Columbia, Vancouver, British Columbia V6T 1Z1, Canada

Received February 4, 2003

The preparation of dipalladium complexes containing sterically nondemanding diphosphine (P–P) ligands of the type $R_2PCH_2PR_2$ where R = Me (dmpm) or Et (depm) is reported. Variable-temperature ^{1}H NMR spectra of the Pd^I_2 complexes $Pd_2X_2(dmpm)_2$ (X = Cl, Br, or I; the P–P ligands in the Pd_2 complexes are always bridged, but for convenience, the μ-symbol is omitted) show the complexes to be fluxional in solution, the barriers to a ring-flipping process being $\Delta G^{\ddagger} = 37.9$, 39.0, and 43.2 ± 0.9 kJ mol^{-1} for the chloro, bromo, and iodo complexes, respectively. Treatment of $Pd_2X_2(P–P)_2$ (X = Cl or Br) with X_2 generates the stable, face-to-face Pd^{II}_2 derivatives *trans*-$Pd_2X_4(P–P)_2$, while oxidation of $Pd_2I_2(P–P)_2$ complexes with I_2 generates a new type of symmetrically di-iodo-bridged, five-coordinate complexes $Pd_2I_2(\mu\text{-}I)_2(dmpm)_2$ and $Pd_2I_2(\mu\text{-}I)_2(depm)_2$. The molecular crystal structures of four dipalladium(II) complexes are described: *trans*-$Pd_2Cl_4(dmpm)_2$·2$CHCl_3$, *trans*-$Pd_2Br_4(dmpm)_2$, *trans*-$Pd_2Cl_4(depm)_2$, and $Pd_2I_2(\mu\text{-}I)_2(dmpm)_2$. Solution NMR and UV–vis absorption spectra are consistent with the solid-state structures determined by X-ray diffraction. The stability of the dimeric Pd(II) complexes is attributed primarily to ligand steric factors.

Introduction

The chemistry of Pd^I is largely based upon coordination by appropriate bidentate tertiary diphosphine (P−P) ligands, especially bis(diphenylphosphino)methane (dppm) and related "short-bite" ligands.[1] Known Pd^I_2 complexes invariably contain a Pd−Pd bond, and significant interest has arisen in the interactions of such species with small molecules of industrial and biological relevance. Of particular interest to us have been the stoichiometric[2,3] and catalytic[4,5] reactions of $Pd_2X_2(dppm)_2$ (X = halogen; throughout the text, the P−P ligands in the Pd_2 complexes are always bridged, but for convenience, the μ-symbol is omitted) with H_2S, which yield bridged-sulfide A-frame complexes and H_2.

Some investigations have focused on Pd^I complexes containing the more basic and sterically nondemanding ligands bis(dimethylphosphino)methane (dmpm) and bis(diethylphosphino)methane (depm).[6−13] Although these complexes resemble the well-known $Pd_2X_2(dppm)_2$ analogues in some respects, modification of steric and electronic ligand properties can significantly alter reactivity; for example, $Pd_2Cl_2(dmpm)_2$ (**1a**) exhibits a much wider range of reactivity than $Pd_2Cl_2(dppm)_2$ and is also water-soluble unlike the dppm species.[6−13] We were interested in extending the H_2S chemistry to aqueous systems, and so, we initiated studies on **1a** and the corresponding depm complex (**2a**) that has

* To whom correspondence should be addressed. E-mail: brj@chem.ubc.ca.
† Deceased October 27, 1998.

(1) Mague, J. T. *J. Cluster Sci.* **1995**, *6*, 217.
(2) (a) Lee, C.-L.; Besenyei, G.; James, B. R.; Nelson, D. A.; Lilga, M. A. *J. Chem. Soc., Chem. Commun.* **1985**, 1175. (b) Besenyei, G.; Lee, C.-L.; Gulinski, J.; Rettig, S. J.; James, B. R.; Nelson, D. A.; Lilga, M. A. *Inorg. Chem.* **1987**, *26*, 3622.
(3) James, B. R. *Pure Appl. Chem.* **1997**, *69*, 2213.
(4) Wong, T. Y. H.; Barnabas, A. F.; Sallin, D.; James, B. R. *Inorg. Chem.* **1995**, *34*, 2278.
(5) Wong, T. Y. H.; James, B. R.; Wong, P. C.; Mitchell, K. A. R. *J. Mol. Catal. A: Chem.* **1999**, *139*, 159.
(6) (a) Kullberg, M. L.; Kubiak, C. P. *Inorg. Chem.* **1986**, *25*, 26. (b) Ni, J.; Kubiak, C. P. *Inorg. Chim. Acta* **1987**, *127*, L37.
(7) (a) Davies, J. A.; Dutremez, S.; Pinkerton, A. A.; Vilmer, M. *Organometallics* **1991**, *10*, 2956. (b) Kluwe, C.; Davies, J. A. *Organometallics* **1995**, *14*, 4257.
(8) Kullberg, M. L.; Kubiak, C. P. *Organometallics* **1984**, *3*, 632.
(9) Kullberg, M. L.; Lemke, F. R.; Powell, D. R.; Kubiak, C. P. *Inorg. Chem.* **1985**, *24*, 3589.
(10) Davies, J. A.; Dutremez, S.; Vilmer, M. *J. Prakt. Chem.* **1992**, *334*, 34.
(11) Kirss, R. U. *J. Coord. Chem.* **1995**, *35*, 281.
(12) Azam, K. A.; Ferguson, G.; Ling, S. S. M.; Parvez, M.; Puddephatt, R. J.; Srokowski, D. *Inorg. Chem.* **1985**, *24*, 2799.
(13) Manojlovic-Muir, L.; Lloyd, B. R.; Puddephatt, R. J. *J. Chem. Soc., Dalton Trans.* **1987**, 201

10.1021/ic030048o CCC: $25.00
Published on Web 05/31/2003

Chart 1. Structures of Complexes **1**−**6**

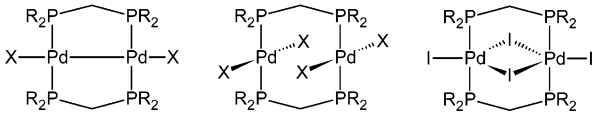

1 (R = Me); **2** (R = Et)
a (X = Cl); **b** (X = Br); **c** (X = I)

3 (R = Me); **4** (R = Et)
a (X = Cl); **b** (X = Br)

5 (R = Me); **6** (R = Et)

not been reported previously. This paper reports our general findings on the $Pd_2X_2(P-P)_2$ species (X = halogen, P−P = dmpm or depm) and their oxidation with halogens; such oxidations have been used previously to remove the bridged-sulfide from $Pd_2X_2(\mu\text{-S})(dppm)_2$ species.[4,14] Chart 1 summarizes the structural types discussed in this paper. Our studies show that modification of the P−P ligand influences greatly the nature and stability of complexes formed via halogen oxidation of the $Pd_2X_2(P-P)_2$ complexes. Studies on the reactions of the $Pd_2X_2(P-P)_2$ complexes with H_2S, CS_2 and COS are ongoing[15] and will be reported later.

Results and Discussion

Dipalladium(I) Complexes. $Pd_2Cl_2(dmpm)_2$ (**1a**) was first prepared by Kubiak's group via reaction of dmpm with $[PdCl(CO)]_n$,[8,9] while an improved synthesis was reported later using dmpm and $Pd_2Cl_2(dppm)_2$.[10] Although the reaction of **1a** with NaBr yields $Pd_2Br_2(dmpm)_2$ (**1b**) in high yield,[8] attempts to prepare $Pd_2I_2(dmpm)_2$ (**1c**) via a similar halide exchange gave unsatisfactory yields.[11] Our attempts to optimize this method gave **1c** contaminated with $Pd_2I_2(\mu\text{-}I)_2(dmpm)_2$ (**5**) (vide infra). An improved method for the synthesis of **1c** involves the reaction of $Pd_2I_2(dppm)_2$ with 2 equiv of dmpm; monitoring this reaction in $CDCl_3$ by $^{31}P\{^1H\}$ NMR spectroscopy indicates quantitative formation of **1c** (δ_P −39.0) and free dppm (δ_P −22.0) after ∼1 h.

An efficient route to $Pd_2Cl_2(depm)_2$ (**2a**) involves the well-known[16] conproportionation of $Pd_2(dba)_3{\cdot}CHCl_3$ and 2 equiv of $PdCl_2(PhCN)_2$ in refluxing acetone or CH_2Cl_2 solutions containing depm (4 equiv). The $^{31}P\{^1H\}$ NMR spectrum of the crude reaction mixture shows that **2a** is the only metal phosphine complex formed, and it is isolated in high yield. Of note, the formation of monomeric $PdCl_2(depm)$ is not observed, although this species has been prepared independently from $PdCl_2(PhCN)_2$ and depm.[12] Complex **2a** is considerably less hygroscopic than **1a** and can be stored in air for several days with no decomposition. The bromo and iodo analogues $Pd_2X_2(depm)_2$ (X = Br (**2b**), I (**2c**)) are conveniently prepared from high yield metathesis reactions. Halide metathesis using less than 2 equiv of NaBr or NaI results in the generation of the mixed halide complexes $Pd_2Cl(X)(dmpm)_2$ (X = Br (**1b′**), I (**1c′**)) that are also formed in situ (in about statistical amounts) when equimolar amounts of **1a** are dissolved in CD_2Cl_2 with **1b** (or **1c**). The $^{31}P\{^1H\}$ NMR spectrum of a solution containing **1a**, **1c**, and **1c′** is shown in Figure 1. These species give broad signals at room temperature (rt, ∼20 °C) but at low temperature are resolved as AA′BB′ multiplets located between the singlet resonances of **1a** and **1b** (or **1c**).

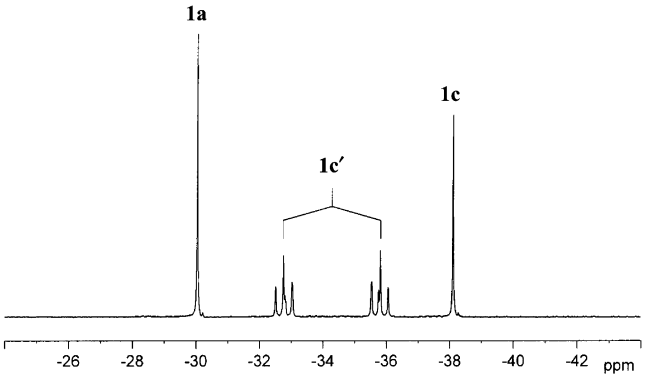

Figure 1. $^{31}P\{^1H\}$ NMR spectrum (121.49 MHz, CD_2Cl_2, 190 K) of the solution obtained by dissolving equimolar amounts of $Pd_2Cl_2(dmpm)_2$ (**1a**) and $Pd_2I_2(dmpm)_2$ (**1c**) in CD_2Cl_2.

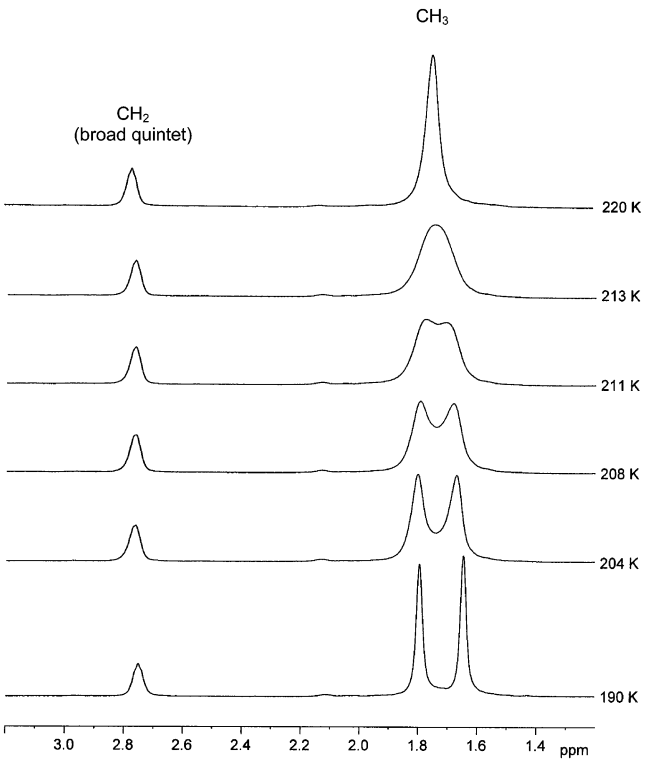

Figure 2. Variable-temperature ^1H NMR spectra (300.13 MHz, CD_2Cl_2) of $Pd_2I_2(dmpm)_2$ (**1c**). Reversible coalescence of the methyl singlets occurs at 213 K.

Fluxionality of the Pd^I_2 Complexes. When a CD_2Cl_2 solution of **1a** is cooled to 190 K, the broad Me resonance of the dmpm ligand undergoes reversible decoalescence, and two broad but distinct Me peaks are resolved at lower temperatures. Complexes **1b** and **1c** exhibit similar dynamic behavior, with coalescence temperatures (T_c) of 200 and 213 K, respectively, determined by ^1H (or $^1H\{^{31}P\}$) NMR spectroscopy; $^1J_{HP}$ coupling is not observed. The reversible, variable-temperature ^1H NMR spectra of **1c** in CD_2Cl_2 are shown in Figure 2. The free energies of activation for the fluxional process are estimated as $\Delta G_c^{\ddagger} = 37.9 \pm 0.9$ (**1a**), 39.0 ± 0.9 (**1b**) and 43.2 ± 0.7 (**1c**) kJ mol^{-1}. ($\Delta G_c^{\ddagger}$ values

(14) Wong, T. Y. H.; Rettig, S. J.; James, B. R. *Inorg. Chem.* **1999**, *38*, 2143.
(15) Pamplin, C. B. Ph.D. Dissertation, University of British Columbia, Vancouver, 2001.
(16) Benner, L. S.; Balch, A. L. *J. Am. Chem. Soc.* **1978**, *100*, 6099.

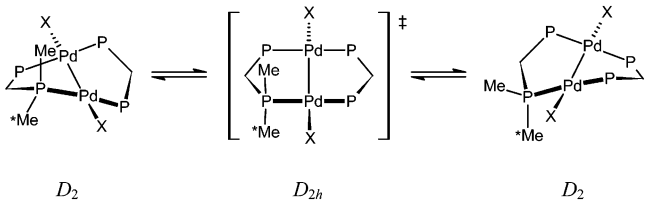

Figure 3. Proposed "ring-flipping" mechanism for the conformational exchange in the Pd(I) complexes. The asterisk indicates an arbitrarily labeled Me group undergoing reversible axial to equatorial conversion via a planar transition state; approximate solution symmetries are shown.

in kJ mol^{-1} were calculated from the coalescence temperature (T_c) and the frequency difference ($\delta\nu$) between the coalescing signals using the formulas $k = \pi\cdot\delta\nu/2^{1/2}$ and $\Delta G_c^{\ddagger} = aT_c[10.319 + \log(T_c/k)]$ where $a = 1.914 \times 10^{-2}$.[17]) Attempts to obtain $\Delta H^{\ddagger}$ and $\Delta S^{\ddagger}$ values for the dynamic process were unsuccessful; the frequency difference $\Delta\nu$ between the exchanging sites is small, and large systematic errors (especially in $\Delta S^{\ddagger}$) are therefore unavoidable.[17]

The solid-state structure of **1b** shows a twist-boat geometry,[9] and the low temperature ^{1}H NMR data for the Pd^I_2 complexes correspond to such a conformation of approximate D_2 symmetry in which the Me groups of each dmpm ligand assume pseudoaxial or pseudoequatorial positions on the $Pd_2P_4C_2$ metallacyclic ring; a rapid "ring-flipping" equilibrium would explain the single, time-averaged Me resonance generated at ambient temperatures (see Figure 3). The small differences in $\Delta G_c^{\ddagger}$ may reflect accessibility of a planar transition state, with the activation barriers correlating with the trans effect of the halogens (I > Br > Cl) that is accompanied by Pd−Pd bond lengths decreasing marginally in the order Cl > Br > I,[18] but it is not clear how such a trend translates to a more accessible planar transition state. A decrease in the P−Pd−Pd−P torsion angle (φ) might realize such accessibility, but this is generally accompanied by an increase in the Pd−Pd bond length for such compounds.[18] Alternatively, the increasing trend in $\Delta G_c^{\ddagger}$ values might relate to moving increasingly larger halogen atoms to achieve the transition state. The substantial energy barrier to the ring-flipping is presumably due to the $Pd_2P_4C_2$ ring having to pass through the strained planar configuration ($\varphi = 0$) with interacting Me groups on adjacent P-atoms, and for such geometry, there is unfavorable overlap of antibonding metal-dπ orbitals.

In comparison with the simple Me resonances in the ^{1}H NMR, the corresponding spectra of the more extensively studied $Pd_2X_2(dppm)_2$ complexes are less informative because of the complex phenyl signals. A dramatic temperature dependence of the $^{31}P\{^1H\}$ chemical shifts of these complexes was correctly attributed to solvation rather than any dynamic process;[19] indeed, the solution fluxionality of these dppm complexes was previously inferred indirectly from the equivalence of the diastereotopic CH_2 protons, where such apparent degeneracy requires rapid exchange brought about by nonrigidity of the $Pd_2P_4C_2$ ring.[18,20]

For Pd^I_2 complexes such as **1** and **2**, the CH_2 resonance of the P−P ligand appears at room temperature (rt) as a 1:4:6:4:1 quintet with apparent J_{PH} coupling of ∼4 Hz, the quintet being due to "virtual coupling" to four equivalent P nuclei.[20,21] Strictly, at low temperature, **1** and **2** generate ABXX′X″X‴A′B′ (A and B = H, X = P) spin systems, as the CH_AH_B protons are chemically nonequivalent; time-averaging of these signals via rapid conformational changes in the $Pd_2P_4C_2$ ring gives rise to the simplified AXX′X″X‴ spectra observed experimentally,[20] and this phenomenon is well-known for "$M_2(P-P)_2$" systems with large (ca. 300 Hz) trans $^2J_{PP}$ coupling.[21] Of interest, the CH_2 quintet in the rt ^{1}H NMR spectra of **1** broadens as the solution temperature is lowered and, even at ∼200 K, is seen as one broad "4H" singlet (Figure 2), while the frozen D_2 structure illustrated in Figure 3 predicts a theoretical CH_AH_B system. Of note, the $^{31}P\{^1H\}$ NMR chemical shifts and line shapes of **1a**−**c** (and **2**) are not temperature-dependent, and only sharp singlets are observed from 180 to 300 K. That the four P atoms maintain equivalence shows that phosphine dissociation plays no role in the fluxional process.

The variable-temperature ^{1}H NMR spectra for $Pd_2Cl_2(depm)_2$ (**2a**) are similar to those of **1** in behavior of the μ-CH_2 resonance (a quintet at rt that broadens to a single resonance at 200 K, see Figure S1). The Me resonance at rt appears as a broad doublet of triplets at δ 1.16 that converts to a well resolved triplet in the $^1H\{^{31}P\}$ spectrum ($^3J_{HH}$ = 7.5 Hz); as the temperature is decreased, coalescence behavior analogous to that shown for **1a** in Figure 2 is seen, and at 200 K, resolution of the axial and equatorial Me groups to two triplets is seen in the $^1H\{^{31}P\}$ spectrum (Figure S1). The ring-flipping mechanism shown in Figure 3 again seems applicable. However, the behavior is more complex in that the rt, 16H multiplet at δ 2.07 seen for the ethyl-CH_2 ^{1}H NMR resonance broadens into the baseline at ∼240 K and then resolves at ∼200 K into three broad multiplets in the δ 1.8−2.4 region integrating for roughly 8, 4, and 4 protons; the $^1H\{^{31}P\}$ NMR spectra are identical to the P-coupled spectra (Figure S1), and so, this pattern must result from geminal ($^2J_{HH}$) and vicinal ($^3J_{HH}$) coupling within an ABX_3 pattern for two sets of inequivalent CH_2 protons that we have been unable to simulate.

Reactions of Dipalladium(I) Complexes with Halogens. The reactions of **1a** or **2a** with 1 equiv of Cl_2 yield the stable complexes *trans*-$Pd_2Cl_4(P-P)_2$; P−P = dmpm (**3a**), and P−P = depm (**4a**). ORTEP diagrams depicting **3a**·2$CHCl_3$ and **4a** are shown in Figures 4 and 5, respectively, and selected bond distances and angles appear in Tables 1 and 2. In both complexes, the dipalladium framework is supported by two mutually trans bridging phosphine ligands, with Pd···Pd distances of 3.3515(5) and 3.3356(4) Å, respectively. Both

(17) Sandström, J. *Dynamic NMR Spectroscopy*; Academic Press: London, 1982; p 96.
(18) Besenyei, G.; Párkányi, L.; Gáes-Baitz, E.; James, B. R. *Inorg. Chim. Acta* **2002**, *327*, 179.
(19) (a) Hunt, C. T.; Balch, A. L. *Inorg. Chem.* **1982**, *21*, 1641. (b) Cyr, P. W.; Patrick, B. O.; James, B. R. *Chem. Commun.* **2001**, 1570.
(20) Balch, A. L.; Benner, L. S.; Olmstead, M. M. *Inorg. Chem.* **1979**, *18*, 2996.
(21) Balch, A. L. In *Homogeneous Catalysis with Metal Phosphine Complexes*; Pignolet, L. H., Ed.; Plenum Press: New York, 1983; p 183.

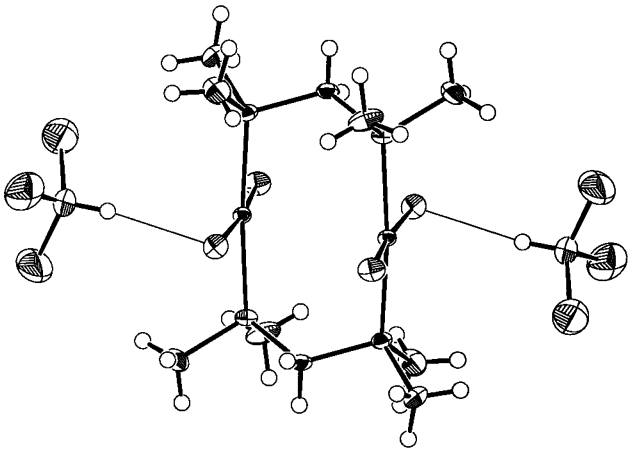

Figure 4. ORTEP diagram of *trans*-$Pd_2Cl_4(dmpm)_2 \cdot 2CHCl_3$ (**3a**·$2CHCl_3$) showing 50% probability thermal ellipsoids and the H-bonding interactions with $CHCl_3$ solvate molecules. The numbering scheme is equivalent to that shown for **3b** (vide infra).

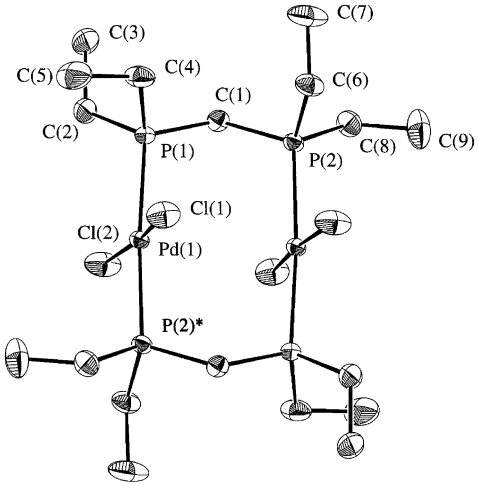

Figure 5. ORTEP diagram of *trans*-$Pd_2Cl_4(depm)_2$ (**4a**) showing 50% probability thermal ellipsoids.

centrosymmetric structures have a crystallographic inversion center located midway between the two Pd atoms. The $Pd_2P_4C_2$ rings of **3a** and **4a** assume chair conformations, and the Pd atoms are found in the familiar square planar coordination environments. The $Pd^{II}-Cl$ bond lengths in **3a** and **4a** are ~0.05 Å shorter than those found in $PdCl_2(dppm)$ (2.362(1) and 2.352(1) Å), while the $Pd^{II}-P$ bond lengths are ~0.07 Å longer than those in the same complex (2.234(1) and 2.250(1) Å),[22] these trends being in line with the trans influence of the phosphine (vs Cl) ligands.[23] Within **3a**, the $CHCl_3$ solvates are H-bonded to a chloro ligand.

The reaction of $PdCl_2(PhCN)_2$ with dmpm provides insoluble di- or polymeric materials, and not monomeric P,P-chelate complexes,[12] while crystals of *cis*-$Pd_2Cl_4(dmpm)_2$ (*cis*-**3a**) were serendipitously isolated by Davies et al. from an $MeNO_2$ solution of $Pd_2Cl_2(dmpm)_2$ (**1a**);[24] the longer Pd−Cl (2.360(1) and 2.353(1) Å) and shorter Pd−P (2.264(1)

Table 1. Selected Bond Lengths (Å) with Estimated Standard Deviations in parentheses

		3a	
Pd(1)−Cl(1)	2.2988(9)	Pd(1)−Cl(2)	2.3053(9)
Pd(1)−P(1)	2.3098(9)	Pd(1)−P(2)[a]	2.3171(9)
Pd···Pd[a]	3.3515(5)	C···Cl (of $Cl_3C-H\cdots Cl$)	3.492(4)
		3b	
Pd(1)−Br(1)	2.4353(8)	Pd(1)−Br(2)	2.4312(8)
Pd(1)−P(1)	2.320(2)	Pd(1)−P(2)[b]	2.314(2)
Pd···Pd[b]	3.350(1)		
		4a	
Pd(1)−Cl(1)	2.3076(8)	Pd(1)−Cl(2)	2.3063(8)
Pd(1)−P(1)	2.3224(7)	Pd(1)−P(2)[c]	2.3171(7)
Pd···Pd[c]	3.3356(4)		
		5[d]	
Pd(1)−I(1)	2.7953(13)	Pd(2)−I(1)	2.8279(12)
Pd(1)−I(2)	2.8602(12)	Pd(2)−I(2)	2.9040(14)
Pd(1)−I(3)	2.6773(13)	Pd(2)−I(4)	2.6677(13)
Pd−P	2.304(4)−2.309(3)	Pd(1)···Pd(2)	2.9075(14)

[a] Refers to the symmetry operation $^1/_3 - x$, $^2/_3 - y$, $^2/_3 - z$. [b] Refers to the symmetry operation $-x$, $1 - y$, $1 - z$. [c] Refers to symmetry operation $1 - x$, $-y$, $1 - z$. [d] Data for one molecule only.

and 2.265(1) Å) bond lengths in *cis*- versus *trans*-**3a** are consistent with the relative trans influence of P and Cl ligands. The P−Pd−P bond angle of 100.67(5)° in *cis*-**3a** is less acute by 27 ± 2° than the corresponding angles in several $PdX_2(P-P)$ complexes (X = halogen) containing chelating bis(dialkylphosphino)methane ligands,[22,25,26] attesting to the relief in ring strain that accompanies a switch from chelating to bridging coordination. The P−C−P bond angle (119.3(3)° in *cis*-**3a**) within the dmpm ligand is identical to that in *trans*-**3a**. Within depm systems, $PdCl_2(depm)$ has been synthesized,[13] but no structural data are available.

Dipalladium(II) complexes, containing $Ph_2P(CH_2)_nPPh_2$ ligands where $n = 5$ or 6, structurally related to **3a** and **4a**, have been prepared via the reaction of $PdCl_2(PhCN)_2$ with the appropriate phosphine ligand, and the structurally characterized *trans*-$Pd_2Cl_4(dpph)_2$ (dpph = 1,6-bis(diphenylphosphino)hexane) has geometry at the Pd atoms similar to that of **3a** and **4a**.[27] In contrast, when $n = 2$ or 3, only monomeric P,P-chelate complexes of Pd(II) are formed.[22] Bidentate ligands containing heavier As and Sb donor atoms also exhibit a reduced tendency toward chelate formation; the synthesis of *trans*-$PdCl_2(\eta^1\text{-dpam})_2$ (dpam = bis(diphenylarsino)methane) has been documented,[28] and the corresponding Sb ligand (dpsm) reacts with $PdCl_2(PhCN)_2$ to yield *trans*-$PdCl_2(\eta^1\text{-dpsm})_2$ and a dimeric product formulated as $[PdCl_2(dpsm)]_2$.[29]

Treatment of **1b** or **2b** with 1 equiv of Br_2 provides **3b** or **4b**, the bromo analogues of **3a** and **4a**. An ORTEP diagram of **3b** is shown in Figure 6, and selected bond lengths and angles are shown in Tables 1 and 2, respectively. The

(22) Steffen, W. L.; Palenik, G. J. *Inorg. Chem.* **1976**, *15*, 2432.
(23) Appleton, T. G.; Clark, H. C.; Manzer, L. E.; *Coord. Chem. Rev.* **1973**, *10*, 335.
(24) Davies, J. A.; Pinkerton, A. A.; Vilmer, M. *Acta Crystallogr.* **1991**, *C47*, 2092.
(25) Peters, K.; Peters, E. M.; VonSchnering, H. G.; Abicht, H. P. Z. *Z. Krystallogr.* **1984**, *168*, 149.
(26) Schmidt, U.; Ilg, K.; Werner, H. *J. Chem. Soc., Dalton Trans.* **2000**, 1005.
(27) Housecroft, C. E.; Shaykh, B. A. M.; Rheingold, A. L.; Haggerty, B. S. *Inorg. Chem.* **1991**, *30*, 125.
(28) Chiffey, A. F.; Evans, J.; Levason, W.; Webster, M. *Polyhedron* **1996**, *15*, 591.
(29) Pringle, P. G.; Shaw, B. L. *J. Coord. Chem.* **1974**, *4*, 47.

Table 2. Selected Bond Angles (deg) with Estimated Standard Deviations in Parentheses

3a			
Cl(1)−Pd(1)−Cl(2)	173.90(4)	Cl(1)−Pd(1)−P(1)	92.17(3)
Cl(1)−Pd(1)−P(2)[a]	87.43(3)	Cl(2)−Pd(1)−P(1)	87.94(3)
Cl(2)−Pd(1)−P(2)[a]	93.01(3)	P(1)−Pd(1)−P(2)[a]	174.88(4)
Pd(1)−P(1)−C	113.34(11)−116.06(12)	Pd(1)[a]−P(2)−C	107.64(11)−118.19(13)
C−P−C	101.1(2)−106.9(2)	P(1)−C(1)−P(2)	119.4(2)
Cl_3C−H···Cl	172.6		
3b			
Br(1)−Pd(1)−Br(2)	168.34(3)	Br(1)−Pd(1)−P(1)	92.28(5)
Br(1)−Pd(1)−P(2)[b]	88.33(4)	Br(2)−Pd(1)−P(1)	88.35(5)
Br(2)−Pd(1)−P(2)[b]	91.09(5)	P(1)−Pd(1)−P(2)[b]	174.82(6)
Pd(1)−P(1)−C	107.6(2)−118.6(2)	Pd(1)[b]−P(2)−C	112.1(2)−117.2(2)
C−P−C	101.6(3)−104.8	P(1)−C(1)−P(2)	119.4(3)
4a			
Cl(1)−Pd(1)−Cl(2)	173.08(3)	Cl(1)−Pd(1)−P(1)	92.36(2)
Cl(1)−Pd(1)−P(2)[c]	87.15(3)	Cl(2)−Pd(1)−P(1)	88.40(3)
Cl(2)−Pd(1)−P(2)[c]	92.60(2)	P(1)−Pd(1)−P(2)[c]	175.69(3)
Pd−P−C	110.52(8)−116.09(10)	C−P−C	101.79(13)−107.67(13)
P(1)−C(1)−P(2)	119.53(13)		
5[d]			
Pd(1)−I(1)−Pd(2)	62.27(3)	Pd(1)−I(2)−Pd(2)	60.58(3)
I(1)−Pd(1)−I(2)	119.82(4)	I(1)−Pd(1)−I(3)	128.84(4)
I(2)−Pd(1)−I(3)	111.29(4)	I(1)−Pd(1)−P(1)	89.88(9)
I(1)−Pd(1)−P(3)	91.88(10)	I(2)−Pd(1)−P(1)	90.87(9)
I(2)−Pd(1)−P(3)	93.21(8)	I(3)−Pd(1)−P(1)	86.96(9)
I(3)−Pd(1)−P(3)	87.48(9)	P(1)−Pd(1)−P(3)	174.02(12)
I(1)−Pd(2)−I(2)	117.23(4)	I(1)−Pd(2)−I(4)	127.74(5)
I(2)−Pd(2)−I(4)	114.99(4)	I(1)−Pd(2)−P(2)	90.07(9)
I(1)−Pd(2)−P(4)	93.20(9)	I(2)−Pd(2)−P(2)	90.80(10)
I(2)−Pd(2)−P(4)	91.67(10)	I(4)−Pd(2)−P(2)	87.29(9)
I(4)−Pd(2)−P(4)	87.18(9)	P(2)−Pd(2)−P(4)	174.46(13)
Pd−P−C	113.2(4)−117.0(4)	C−P−C	98.6(7)−106.9(7)
P(1)−C(1)−P(2)	119.6(5)		

[a−d] Footnotes as in Table 1.

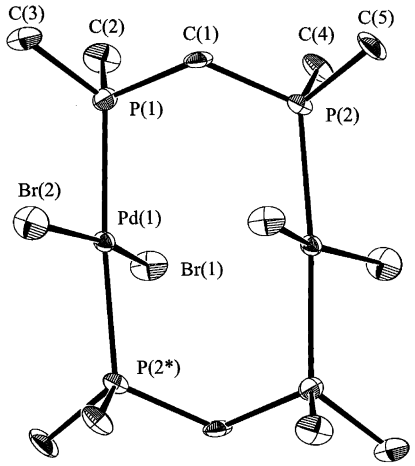

Figure 6. ORTEP diagram of *trans*-$Pd_2Br_4(dmpm)_2$ (**3b**) showing 50% probability thermal ellipsoids.

structure of **3b** resembles that of **3a** but crystallizes without H-bonded $CHCl_3$ solvates. The Pd atoms again have close to square planar geometry with trans bromines. The Pd−Br bond lengths in **3b** are shorter than those found in $PdBr_2$(dppm) (2.474(2)−2.488(2) Å),[25] $Pd_2Br_2(dppm)_2$ (2.527(6) and 2.543(6) Å),[30] and **1b** (2.522(1) Å).[9] In addition, the Pd−P bonds in **3b** are longer than those in $PdBr_2$(dppm) (2.225(3)−2.242(4) Å),[25] $Pd_2Br_2(dppm)_2$ (2.29(1), 2.26(1), 2.28(1), and 2.32(1) Å),[30] and **1b** (2.291(3) and 2.275(3) Å).[9] The two Pd atoms in **3b** are separated by 3.350(1) Å. Of note, the X−Pd−X angles in **3a** (and **4a**) and **3b** deviate slightly from linearity (∼173° and 168°, respectively); whether this results from M···M interactions giving rise to steric halogen···halogen interactions[31] is unclear (see also the next section). For example, the Cl(1)−Cl(2)* distance of 3.607 Å in **4a** is essentially twice the van der Waals radius for Cl;[32a] in *trans*-$Pd_2Cl_4(dpph)_2$ (see details earlier in this text), where the Pd−Pd distance is ∼9 Å, the Cl−Pd−Cl angles are 177.5°.[27]

The iodo complex $Pd_2I_2(\mu\text{-}I)_2(dmpm)_2$ (**5**) was first observed as an impurity formed during the attempted synthesis of $Pd_2I_2(dmpm)_2$ (**1c**) from **1a** and NaI; however, addition of excess I_2 to solutions containing mixtures of **1c** and **5** resulted in quantitative oxidation to the latter species. Analytically pure **5** and the depm analogue $Pd_2I_2(\mu\text{-}I)_2(depm)_2$ (**6**) were independently isolated from the reaction of I_2 with **1c** or **2c**, respectively. An ORTEP diagram showing one molecule of **5** is shown in Figure 7 (the asymmetric unit cell contains 2.5 molecules), and selected bond distances and angles appear in Tables 1 and 2, respectively. Each Pd atom is located in a trigonal bipyramidal coordination environment with axial P-atoms and an equatorial plane composed of one terminal and two bridging I-atoms. The terminal Pd−I bond lengths in **5** are consider-

(30) Holloway, R. G.; Penfold, B. R.; Colton, R.; McCormick, M. J. *J. Chem. Soc., Chem. Commun.* **1976**, 485.

(31) Che, C.-M.; Wong, W.-T.; Lai, T.-F.; Kwong, H.-L. *J Chem. Soc., Chem. Commun.* **1989**, 243.

(32) Huheey, J. E. *Inorganic Chemistry: Principles of Structure and Reactivity*, 3rd ed.; Harper & Row: New York, 1983; (a) p 292, (b) p 436.

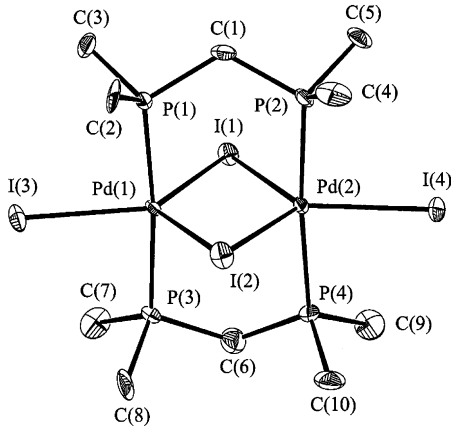

Figure 7. ORTEP view of one molecule of $Pd_2I_2(\mu\text{-}I)_2(dmpm)_2$ (**5**) showing 50% probability thermal ellipsoids; the asymmetric unit contains 2.5 molecules of **5**, each possessing a unique geometry.

ably shorter than the bridging Pd−I bond lengths and are marginally longer than those found in $PdI_2(dppm)$ (2.6514(4) and 2.6519(4) Å)[33] and *trans*-$Pd_2I_4(dpam)_2$ (2.6217(10) and 2.6395(10) Å).[34] In the latter complex, one of the terminal iodines interacts weakly with an adjacent Pd atom (Pd···I = 3.1562(11) Å),[34] and so, the complex has a geometry "intermediate" between that of *trans*-$Pd_2X_4(P-P)_2$ and $Pd_2X_2(\mu\text{-}X)_2(P-P)_2$ species. The Pd−P bond lengths in **5** are correspondingly longer than those in $PdI_2(dppm)$ (2.241(1) and 2.2525(9) Å)[33] and much shorter than the average Pd−As bond length in *trans*-$Pd_2I_4(dpam)_2$ (2.392(8) Å).[34] These trends are consistent with the established trans influence and the enhanced π-accepting tendency of P relative to As.[32b] Complex **5**, with two "real" bridging iodines, is the first of its type to be structurally characterized. That μ-I(2) exhibits longer Pd−I distances (by 0.06 Å) than does μ-I(1), with corresponding I(terminal)−Pd−I(2) angles being 12−18° more acute than those involving I(1), likely results from a solid-state effect in that I(1) is 3.72 Å from the nearest C atom of a neighboring molecule, while for I(2) the distance is 3.98 Å, the van der Waals radii for I and CH_3 (or CH_2) both being ∼2.0 Å.[32a] That the I-system exists as the dibridged complex rather than the open trans isomers (cf. the Cl and Br systems) presumably reflects the better bridging capability of the larger, more polarizable iodide ligand.

The Pd−Pd distances in molecules of **5** (2.8842(13)−2.926(2) Å) are much shorter than those found in *trans*-**3a**, -**3b**, and -**4a**, and *trans*-$Pd_2I_4(dpam)_2$ (3.336(1)−3.515(5) Å),[34] and indeed are within the range accepted for Pd−Pd σ-bonds.[35] Although a Pd−Pd interaction is usually not evident between two 18e Pd(II) centers, the possibility of a weak Pd−Pd interaction cannot be ruled out (see next section). Unlike the chair conformations found in the metallacycles of *trans*-**3a**, -**3b**, and -**4a**, the $Pd_2P_4C_2$ ring of **5** assumes a highly symmetric boat conformation; the terminal iodide ligands are oriented toward one of the bridged-iodides such that the dihedral angle between the planes defined by I(3)−Pd(1)−P(1)−P(3) and I(4)−Pd(2)−P(2)−P(4) is 165.6°. The somewhat oddly shaped ellipsoids, shown for example for C(2) and C(8), and some large residual electron density peaks in the final difference map, are thought to be due to an inadequate absorption correction.

Five-coordinate intermediates similar to **5** or **6** were invoked, but not detected, in the fragmentation of *trans*-$Pd_2X_4(dppm)_2$, generated in situ at low temperature, to $PdX_2(dppm)$.[14,36] The structural data reported here corroborate suggestions by Hunt and Balch that formation of halide bridges occurs prior to Pd−P bond breaking.[36] An alternate mechanism involving direct Pd−P bond rupture is unlikely given the preference for associative substitution reactions at d^8 metal centers. The driving force for chelate ring formation in the Pd(II)−dppm complexes appears to be directly related to the relative stability of the resulting four-membered Pd−P−C−P chelate ring. In contrast, complexes that contain sterically nondemanding substituents on the phosphine ligands (complexes **3**−**6**) are more thermally stable and evidently do not undergo fragmentation. The five-coordinate Pt(II) intermediate $Pt_2Me_2(\mu\text{-}I)_2(dmpm)_2$ has been invoked to rationalize the solution fluxionality of *trans*-$Pt_2I_2Me_2(dmpm)_2$ that, like **3** and **4**, possesses a "face-to-face" geometry in the solid state.[37]

The rt ^1H NMR spectra of **3**−**6** reveal the expected quintet for the μ-CH_2, and "standard" resonances for the Me and CH_2 (for the depm systems) of the P−alkyl moieties, although coupling of the Me resonance to the P atom of dmpm was not resolved. The solid-state structures of **5** and presumably **6** are maintained in CH_2Cl_2; **5** is essentially nonconducting in this solvent.

Electronic Absorption Spectra. The "face-to-face" Pd^{II}_2 complexes **3** and **4** are yellow or orange, while the five-coordinate **5** and **6** are dark purple in the solid state and violet in $CHCl_3$ solution. The UV−vis spectra of **3a**, **3b**, and **5** are shown in Figure 8, and all the spectral data are given in the Experimental Section. The spectra of **3a** and **4a** exhibit a single strong transition with a distinct shoulder; band assignment is aided by comparison with the electronic spectra of the bromo complexes **3b** and **4b**, for which the λ_{max} values are red-shifted by ∼30 nm. The energy ordering of these bands is typical of LMCT (halogen → Pd) for square planar d^8 complexes, which typically feature a single, strong absorption band.[38] The $[PdX_4]^{2-}$ species (X = Cl, Br) in aq HX exhibit two charge transfer bands, with ϵ values in the range $(1.0-3.0) \times 10^4$ M^{-1} cm^{-1}, at 223 and 278 nm for X = Cl, and at 247 and 332 nm for the Br system.[39] We feel that the relatively simple electronic spectra of **3** and **4** are

(33) Davies, J. A.; Pinkerton, A. A.; Syed, R.; Vilmer, M. *J Chem. Soc., Chem. Commun.* **1988**, 47.
(34) Zhang, T.; Drouin, M.; Harvey, P. D. *J. Chem. Soc., Chem. Commun.* **1996**, 877.
(35) Lin, W.; Wilson, S. R.; Girolami, G. S. *Inorg. Chem.* **1994**, *33*, 2265.
(36) Hunt, C. T.; Balch, A. L. *Inorg. Chem.* **1981**, *20*, 2267.
(37) Manojlovic-Muir, L.; Ling, S. S. M.; Puddephatt, R. J. *J. Chem. Soc., Dalton Trans.* **1986**, 151.
(38) Lever, A. B. P. *Inorganic Electronic Specroscopy*; Elsevier Science Publishers: New York, 1984; p 534.
(39) (a) Day, P.; Orchard, A. F.; Thompson, A. J.; Williams, R. J. P. *J. Chem. Phys.* **1965**, *42*, 1973. (b) Basch, H.; Gray, H. B. *Inorg. Chem.* **1967**, *6*, 365. (c) Gray, H. B.; Ballhausen, C. J. *J. Am. Chem. Soc.* **1963**, *85*, 260.

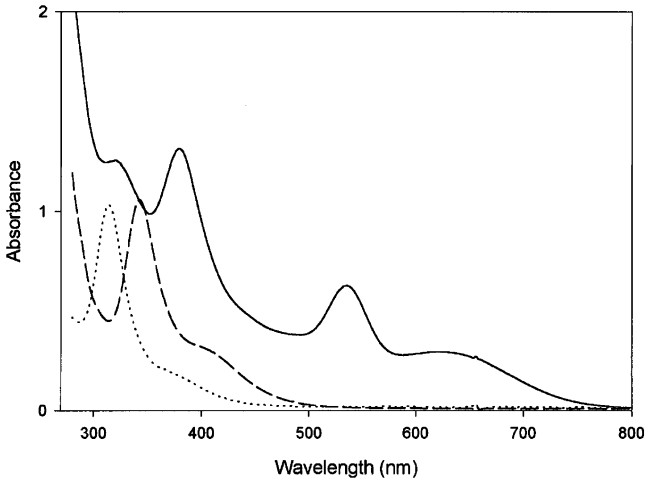

Figure 8. Solution UV−vis spectra (1.0×10^{-4} M in $CHCl_3$) of *trans*-$Pd_2Cl_4(dmpm)_2$ (**3a**, · · ·), *trans*-$Pd_2Br_4(dmpm)_2$ (**3b**, − − −), and $Pd_2I_2(\mu\text{-}I)_2(dmpm)_2$ (**5**, —).

consistent with no metal−metal bonding interactions in solution. This does contrast, however, with conclusions on $Pd_2(dppm)_2(CN)_4$ which has an open trans structure akin to those of **3** and **4**, and a Pd−Pd distance of 3.276 Å, where an intense absorption band at 272 nm was attributed to a weak metal−metal interaction.[40] This was presented as an example of a "proximity effect", documented for other dimetallic, square planar Pt(II),[41] Rh(I),[42−44] and Ir(I)[44] complexes, where there is a shift in the lowest energy charge transfer band to lower energy as the metal−metal interaction increases.

The electronic spectra of **5** and **6** differ greatly from those of **3** and **4**, the presence of two lower energy absorption bands accounting for their violet solutions. Assignment of the LMCT (I → Pd) bands is aided by comparison with known data for the trigonal bipyramidal $NiX_2(PMe_3)_3$ species (X = Cl, Br, I) in which the ligand orbital energies increase according to X = Cl < Br < I.[45] For **5**, the bands at 378 and 320 nm are tentatively ascribed to I(pπ) → Pd and I(pσ) → Pd, respectively, and an intense absorption at λ < 300 nm (also present in **3** and **4**) is assigned to the common transition P(pσ) → Pd. The two lower energy transitions in **5** and **6** are consistent with those observed in the C_{2v} symmetric Ni(II) complexes: these ligand field bands correspond to the $^1A_1 \rightarrow {}^1A_1$ (the latter derived from the $^1E'$ term in D_{3h} symmetry) and the $^1A_1 \rightarrow {}^1B_1$ (derived from the $^1E''$ term in D_{3h} symmetry) transitions.[45] Thus, the following spectral assignments are possible for **5**, which also has approximate C_{2v} symmetry at each Pd atom: 622 nm = $^1A_1 \rightarrow {}^1A_1$ (a_1, $d_{x^2-y^2} \rightarrow a_1$, d_{z^2}), and 534 nm = $^1A_1 \rightarrow {}^1B_1$ (b_1, $d_{xy} \rightarrow a_1$, d_{z^2}). An expected third absorption band, $^1A_1 \rightarrow {}^1B$ (b_2, $d_{xy} \rightarrow a_1$, d_{z^2}), is not observed, which is not surprising considering that the transition, while allowed in C_{2v} symmetry, is derived from an orbitally forbidden $^1A_1 \rightarrow {}^1E''$ transition in D_{3h} symmetry.[45] Indeed, the $^1A_1 \rightarrow {}^1B_2$ transition is not detected in the solution absorption spectrum of C_{2v} symmetric $NiBr_2(PMe_3)_3$ at 22 °C but is observed in the spectrum of a crystalline sample at −196 °C.[45] The absorption bands of **6** are red-shifted slightly with respect to those of **5**, but the spectrum is otherwise very similar.

The addition of excess *n*-Bu_4NI (up to 100 equiv) to solutions of **5** in $CHCl_3$ caused no change in the absorption spectrum of **5**, suggesting that dissociation of I^- does not occur and that five-coordinate geometry persists in solution. Solutions of **5** or **6** can be refluxed in $CHCl_3$ for hours with no decomposition (e.g., to form I_2), and the complexes can be recovered intact.

Attempts to assign the ν(Pd−X) stretching frequencies in the far-IR spectra of **3**−**6** were thwarted by an unusual solid-state halide metathesis reaction with CsI (a suitable matrix). When yellow **3a** or orange **3b** was ground with CsI, the samples became purple, and that from **3a** generated an IR spectrum identical to that of an authentic sample of **5**. The occurrence of a solid-state reaction was confirmed by extraction of the purple, $CDCl_3$-soluble fraction from the IR sample of **3a**; the UV−vis absorption and ^1H and $^{31}P\{^1H\}$ NMR spectra ($CDCl_3$) were consistent with quantitative formation of **5**. The solid-state Raman spectra of **3a** and **3b** show multiple bands in the 150−350 cm^{-1} range, and assignment of the Pd−X bands was not possible. Attempts to record Raman spectra of **5** were unsuccessful due to strong absorption of incident radiation by the sample.

Conclusions

A series of stable dipalladium(II) halide complexes was prepared by halogen oxidation of $Pd^I_2X_2(P-P)_2$ precursors (X = halogen; P−P = dmpm, depm). The chloro and bromo complexes assume a "face-to-face" coordination geometry, while the analogous iodo species are five-coordinate in solution and in the solid state.

Experimental Section

General. Unless otherwise noted, all synthetic procedures were carried out using standard Schlenk techniques under dry N_2. Reagent grade solvents were distilled under N_2 from the appropriate standard drying agent. CD_2Cl_2 and $CDCl_3$ (Cambridge Isotope Laboratories) were dried over CaH_2 and vacuum transferred into storage vessels containing activated molecular sieves (4 Å) or directly into NMR tubes equipped with J. Young PTFE valves or rubber septa. Of the phosphines, dmpm and dppm were purchased from Strem and used as received, while depm was prepared by a literature method[46] and stored under N_2. Cl_2 (Matheson), Br_2 (Acros), and I_2 (AnalaR) were from commercial sources and used as received. Gastight Sample-Lok syringes (Dynatech) were used for handling gaseous reagents; after the syringe was flushed with the gas, a known quantity (at

(40) Yip, H.-K.; Lai, T.-F.; Che, C.-M. *J. Chem. Soc., Dalton Trans.* **1991**, 1639.
(41) Langrick, C. R.; McEwan, D. M.; Pringle, P. G.; Shaw, B. L. *J. Chem. Soc., Dalton Trans.* **1983**, 2487.
(42) Balch, A. L.; Tulyman, B. *Inorg. Chem.* **1977**, *16*, 2840.
(43) (a) Balch, A. L. *J. Am. Chem. Soc.* **1976**, *98*, 8049. (b) Mann, K. R.; Lewis, N. S.; Williams, R. M.; Gray, H. B.; Gordon, J. G. *Inorg. Chem.* **1978**, *17*, 828. (c) Balch, A. L.; Labadie, J. W.; Delker, G. *Inorg. Chem.* **1979**, *18*, 1224. (d) Fordyce, W. A.; Crosby, G. A. *J. Am. Chem. Soc.* **1982**, *104*, 985.
(44) Mague, J. T.; deVries, S. H. *Inorg. Chem.* **1980**, *19*, 3743.
(45) Dawson, J. W.; McLennan, T. J.; Robinson, W.; Merle, A.; Dartiguenave, M.; Dartiguenave, Y.; Gray, H. B. *J. Am. Chem. Soc.* **1974**, *96*, 4428.
(46) Prishchenko, A. A.; Nifantev, N. E.; Novikova, Z. S.; Lutsenko, I. F. *Zh. Obshch. Khim.* **1980**, *50*, 1881.

Table 3. Crystallographic Data[a]

	3a·2CHCl$_3$	**3b**	**4a**	**5**
empirical formula	$C_{12}H_{30}Cl_{10}P_4Pd_2$	$C_{10}H_{28}Br_4P_4Pd_2$	$C_{18}H_{44}Cl_4P_4Pd_2$	$C_{10}H_{28}I_4P_4Pd_2$
fw	865.59	804.64	739.05	992.64
color, habit	yellow, prism	orange, prism	orange, block	purple, block
cryst size, mm^3	0.25 × 0.30 × 0.30	0.25 × 0.20 × 0.10	0.60 × 0.50 × 0.40	0.45 × 0.30 × 0.15
cryst syst	trigonal	monoclinic	monoclinic	monoclinic
space group	$R\bar{3}$ (No. 148)	$P2_1/n$ (No. 14)	$P2_1/n$ (No. 14)	$P2_1/n$ (No. 14)
a, Å	21.3094(4)	8.7158(12)	10.7360(6)	10.9830(14)
b, Å	21.3094(4)	8.1239(8)	11.667(2)	14.434(2)
c, Å	17.6357(3)	15.8295(5)	11.9135(3)	38.7078(6)
β, deg	90	98.5516(8)	104.3174(5)	93.9489(4)
V, Å^3	6935.3(2)	1108.4(2)	1445.9(2)	6121.6(8)
Z	9	2	2	10
T, K	180	180	293	180
ρ_{calcd}, g/cm^3	1.865	2.411	1.697	2.692
F(000)	3816	760	744	4520
μ, cm^{-1}	22.44	91.34	18.41	67.68
transm factors[b]	0.8298−1.0000	0.5920−1.0000	0.7557−1.0000	0.6107−1.0000
scan type	ϕ, ω sweeps	ϕ, ω sweeps	ϕ, ω sweeps	ϕ, ω sweeps
scan range, deg in ω	0.5	0.5	0.5	0.3
data images	462 exp of 8.0 s	462 exp of 16.0 s	464 exp of 12.0 s	768 exp of 8.0 s
$2\theta_{max}$, deg	61.0	61.0	55.9	61.1
total reflns	20402	9606	11858	55497
unique reflns	4407	2811	3375	15346
R_{int}	0.033	0.040	0.054	0.053
no. with $I \geq 3\sigma(I)$	2904	1933	3148	6125
no. variables	127	92	127	454
$R(F)$ ($I \geq 3\sigma(I)$)	0.054	0.036	0.029	0.044
$R_w(F)$ ($I \geq 3\sigma(I)$)	0.058	0.035	0.062	0.042
$R(F^2)$ (all data)		0.069	0.041	0.090
$R_w(F^2)$ (all data)		0.072	0.105	0.086
gof	1.47	1.78	1.18	1.28
max Δ/σ	0.001	0.0003	0.03	0.098
residual density, e/Å^3	−1.29	−1.73	−1.03	−4.89

[a] Rigaku/ADSC CCD diffractometer, Mo Kα (λ = 0.71069 Å), graphite monochromator, aperture 94 × 94 mm^2 at distances of 38.85(2) mm (for **3a**), 38.859(9) mm (for **3b**), 40.47(2) mm (for **4a**), and 38.889(6) mm (for **5**) from the crystal. All data used in the refinement. Function minimized $\sum w(F_o^2 - F_c^2)^2$ where $w = 1/\sigma^2(F_o^2)$, $R = \sum||F_o| - |F_c||/\sum|F_o|$, $R_w = [\sum w(F_o^2 - F_c^2)^2/\sum(F_o^2)^2]^{1/2}$. [b] Includes crystal decay, absorption, and scaling corrections.

STP) was injected into a septum-sealed reaction vessel or NMR tube. The complexes $Pd_2(dba)_3$·$CHCl_3$,[47] $PdCl_2(PhCN)_2$,[48] $Pd_2I_2(dppm)_2$,[16] and $Pd_2X_2(dmpm)_2$ (X = Cl (**1a**),[10] Br (**1b**)[8,9]) were prepared by reported methods.

NMR spectra were recorded on a Bruker AV300 spectrometer (300.13 MHz for ^{1}H, 121.49 MHz for ^{31}P). Residual deuterated solvent proton (relative to external $SiMe_4$) or external $P(OMe)_3$ (^{31}P, δ 141.0 relative to 85% H_3PO_4) was used as a reference (s = singlet, d = doublet, t = triplet, qn = quintet, dq = doublet of quartets, m = multiplet, br = broad). J values are reported in Hz. UV−vis absorption spectra were recorded on a Hewlett-Packard 8452A diode-array spectrometer, data being presented as λ_{max} (nm) ($\epsilon_{max} \times 10^{-3}$ M^{-1} cm^{-1}). Attempts to measure IR spectra (see Results and Discussion section) were made using CsI pellets with an ATI Mattson Genesis FTIR instrument, and Raman spectra were recorded as pressed powders on a Bruker RFS 100 spectrophotometer using Nd:YAG radiation (λ = 1.064 μm) and calibrated using an S_8 standard. Conductivity measurements were made at 298 K using a model RCM151B Serfass conductance bridge (A. H. Thomas Co. Ltd.) connected to a 3403 cell from the Yellow Springs Instrument Company. The cell was calibrated using a standard 0.01000 M aq KCl solution (Λ_M = 141.3 Ω^{-1} cm^2 mol^{-1} at 298 K), the cell constant being 1.016 cm^{-1}. Elemental analyses were performed by Mr. P. Borda of the UBC Microanalytical Service.

X-ray Crystallographic Analyses. Selected crystallographic data appear in Table 3. More details are provided in the Supporting Information. Suitable crystals of **3a**·2$CHCl_3$, **3b**, **4a**, and **5** were isolated from $CHCl_3$ solutions and mounted on a glass fiber using Paratone-N oil. All measurements were made on a Rigaku/ADSC CCD area detector with graphite monochromated Mo Kα radiation. Crystallographic data were processed using the d*TREK area detector program,[49] and structure solution and refinement calculations were performed using the teXsan crystal structure analysis package.[50] All data were corrected for Lorentz and polarization effects. The structures were solved by direct methods (**3a**·2$CHCl_3$, **3b** and **4a**)[51] or Patterson methods (**5**)[52] and expanded using Fourier techniques.[53] The non-H atoms were refined anisotropically, and H atoms were fixed in calculated positions. There are 2.5 molecules in the asymmetric unit of **5**, one of which is situated at an inversion center, and each molecule possesses a unique geometry. The C atoms of the dmpm ligand of the centrosymmetric molecule are

(47) Ukai, T.; Kawazura, H.; Ishii, Y.; Bonnet, J.; Ibers, J. A. *J. Organomet. Chem.* **1974**, *65*, 253.
(48) Anderson, G. K.; Lin, M. *Inorg. Synth.* **1990**, *28*, 61.
(49) *d*TREK. Area Detector Software*, version 4.13; Molecular Structure Corporation: The Woodlands, TX, 1996−1998.
(50) *teXsan. Crystal Structure Analysis Package*; Molecular Structure Corporation: The Woodlands, TX, 1985 and 1992.
(51) Altomare, A.; Burla, M. C.; Cammalli, G.; Cascarano, M.; Giacovazzo, C.; Guagliardi, A.; Moliterni, A. G. G.; Polidori, G.; Spagna, A. *J. Appl. Crystallogr.* **1999**, *32*, 115.
(52) Beurskens, P. T.; Admiraal, G.; Beurskens, G.; Bosman, W. P.; Garcia-Granda, S.; Gould, R. O.; Smits, J. M. M.; Smykalla, C. *The DIRDIF-92 program system*; Technical Report of the Crystallography Laboratory; University of Nijmegen: Nijmegen, The Netherlands, 1992.
(53) Beurskens, P. T.; Admiraal, G.; Bosman, W. P.; de Gelder, R.; Israel, R.; Smits, J. M. M. *The DIRDIF-94 program system*; Technical Report of the Crystallography Laboratory; University of Nijmegen: Nijmegen, The Netherlands, 1994.

disordered, and this was partially resolved by split-atom refinement of C(21) and C(23); the partial carbon atoms C(21a), C(23), and C(23a) were refined isotropically, while the remaining non-H atoms were refined anisotropically.

Dipalladium(I) Complexes. Improved Synthesis of $Pd_2I_2(dmpm)_2$ (1c). To a solution of $Pd_2I_2(dppm)_2$ (0.117 g, 0.094 mmol) in CH_2Cl_2 (20 mL) was added dmpm (0.026 g, 0.189 mmol) via microsyringe. The violet solution turned orange and was stirred at rt for 2 h. The reaction mixture was then concentrated to ~5 mL prior to the addition of hexanes (20 mL) to initiate the formation of an orange-red solid. The precipitate was isolated, washed with hexanes (2 × 10 mL), and dried in vacuo at rt. Yield: 0.066 g (95%). ^{1}H NMR (CD_2Cl_2): δ 1.81 (br s, 24H, CH_3), 2.82 (qn, 4H, CH_2, J_{PH} = 3.6). ^{1}H{^{31}P} NMR (CD_2Cl_2): δ 1.81 (br s, 24H, CH_3), 2.82 (s, 4H, CH_2). ^{31}P{^{1}H} NMR (CD_2Cl_2): δ −38.1 (s). UV−vis (CH_2Cl_2): 266 sh (19.4), 290 sh (14.6), 358 (15.1), 404 (11.5), 438 sh (9.10). Anal. Calcd for $C_{10}H_{28}I_2P_4Pd_2$: C, 16.26; H, 3.82. Found: C, 16.57; H, 3.88. Complex **1c** was previously isolated in 15% yield from the reaction of **1a** with NaI, and the NMR data here are consistent with reported data.[11]

In Situ Characterization of $Pd_2Cl(X)(dmpm)_2$ (X = Br (1b′), I (1c′)). To a solution of **1a** (3.1 mg, 4.20 μmol) in CD_2Cl_2 (1 mL) was added **1b** (2.7 mg, 4.20 μmol). The orange solution was shaken, and the ^{31}P{^{1}H} NMR spectrum was recorded. ^{31}P{^{1}H} NMR (CD_2Cl_2, 293 K): δ −32.2 (br). ^{31}P{^{1}H} NMR (CD_2Cl_2, 190 K): δ −30.0 (s, **1a**), −31.6 (**1b′**, center of AA′BB′ pattern), −33.0 (s, **1b**).

Similarly, a CD_2Cl_2 solution of **1a** (3.1 mg, 4.20 μmol) reacts with **1c** (2.3 mg, 4.20 μmol) to yield a mixture containing **1a**, **1c′**, and **1c**. ^{31}P{^{1}H} NMR (CD_2Cl_2, 293 K): δ −38.1 (br s), −34.5 (br), −32.5 (br), −30.1 (br). ^{31}P{^{1}H} NMR (CD_2Cl_2, 190 K): δ −30.0 (s, **1a**), −34.3 (**1c′**, center of AA′BB′ pattern), −38.1 (s, **1c**).

$Pd_2Cl_2(depm)_2$ (2a). To an acetone solution (10 mL) of $Pd_2(dba)_3{\cdot}CHCl_3$ (0.199 g, 0.192 mmol) and depm (0.147 g, 0.766 mmol) was added a solution of $PdCl_2(PhCN)_2$ (0.147 g, 0.383 mmol) in acetone (5 mL). The brown suspension was refluxed at 50 °C for 1 h, and the resulting orange solution was then filtered through Celite. The solution was concentrated to 5 mL, and an orange solid was precipitated with hexanes (20 mL). The product was isolated, washed with hexanes (2 × 10 mL), and dried in vacuo at 78 °C. Yield: 0.224 g (87%). ^{1}H NMR ($CDCl_3$): δ 1.16 (m, 24H, CH_2CH_3), 2.07 (m, 16H, CH_2CH_3), 2.51 (qn, 4H, PCH_2P, J_{PH} = 3.7). ^{1}H{^{31}P} NMR ($CDCl_3$): δ 1.16 (t, 24H, CH_2CH_3, $^3J_{HH}$ = 7.5), 2.07 (m, 16H, CH_2CH_3), 2.51 (s, 4H, PCH_2P). ^{31}P{^{1}H} NMR ($CDCl_3$): δ −10.8 (s). UV−vis (CH_2Cl_2): 284 (34.1), 326 (18.2), 392 (7.6). Anal. Calcd for $C_{18}H_{44}Cl_2P_4Pd_2$: C, 32.36; H, 6.64. Found: C, 32.28; H, 6.67.

$Pd_2X_2(depm)_2$ (X = Br, (2b), I (2c)). These complexes were prepared from the halide metathesis reactions of **2a** with NaX (X = Br, I). Thus, a solution of **2a** (0.034 g, 0.051 mmol) in CH_2Cl_2 (8 mL) was treated with a solution of NaBr (0.105 g, 1.02 mmol) in MeOH (5 mL). The reaction mixture was stirred for 8 h, and the solution was evaporated to dryness; the residue was extracted with CH_2Cl_2 (4 × 3 mL) and filtered through Celite. An orange solid, precipitated from the filtrate with addition of hexanes (20 mL), was isolated, washed with hexanes (2 × 5 mL), and dried in vacuo at 78 °C. Yield: 0.025 g (84%). ^{1}H NMR ($CDCl_3$): δ 1.14 (m, 24H, CH_2CH_3), 2.11 (m, 16H, CH_2CH_3), 2.51 (qn, 4H, PCH_2P, J_{PH} = 3.6). ^{31}P{^{1}H} NMR ($CDCl_3$): δ −13.4 (s). UV−vis ($CHCl_3$): 252 (16.6), 286 (24.6), 340 (21.0), 404 (9.6). Anal. Calcd for $C_{18}H_{44}Br_2P_4Pd_2$: C, 28.56; H, 5.86. Found: C, 28.75; H, 6.00.

Similarly, a solution of **2a** (0.101 g, 0.151 mmol) in CH_2Cl_2 (10 mL) reacts with a solution of NaI (0.454 g, 3.03 mmol) in MeOH (10 mL) to yield red-brown **2c**. Yield: 0.102 g (79%). ^{1}H NMR ($CDCl_3$): δ 1.13 (m, 24H, CH_2CH_3), 2.19 (m, CH_2CH_3), 2.60 (qn, 4H, PCH_2P, J_{PH} = 3.7). ^{31}P{^{1}H} NMR ($CDCl_3$): δ −17.5 (s). UV−vis ($CHCl_3$): 258 (20.7), 270 (20.4), 366 (17.0), 420 (12.1), 450 (10.5). Anal. Calcd for $C_{18}H_{44}I_2P_4Pd_2$: C, 25.40; H, 5.21. Found: C, 24.98; H, 5.13.

Dipalladium(II) Complexes. *trans*-$Pd_2Cl_4(P{-}P)_2$ (P−P = dmpm (3a), depm (4a)). To a solution of **1a** (0.062 g, 0.112 mmol) in CH_2Cl_2 (5 mL) was added Cl_2 (2.7 mL, 0.112 mmol). A pale yellow precipitate formed in the mixture, which was stirred for 30 min and then evaporated to ~2 mL. The addition of hexanes (10 mL) completed precipitation of the solid that was isolated, washed with hexanes (2 × 5 mL), and dried in vacuo at 78 °C. Yield of **3a**: 0.059 g (85%). ^{1}H NMR ($CDCl_3$): δ 1.63 (br s, 24H, CH_3), 2.53 (qn, 4H, CH_2, J_{PH} = 4.6). ^{31}P{^{1}H} NMR ($CDCl_3$): δ −6.9 (s). UV−vis ($CHCl_3$): 314 (10.4), 378 sh (2.50). Raman, ν(Pd−Cl) region: 111 (w), 157 (m), 204 (w), 274 (m), 303 (m). Anal. Calcd for $C_{10}H_{28}Cl_4P_4Pd_2$: C, 19.16; H, 4.50. Found: C, 19.57; H, 4.68. Yellow crystals of **3a**·2$CHCl_3$ were grown by slow evaporation of a dilute $CHCl_3$ solution.

Similarly, a solution of **2a** (0.050 g, 0.075 mmol) in CH_2Cl_2 (10 mL) reacts with Cl_2 (1.9 mL, 0.078 mmol) to yield **4a**. Yield: 0.048 g (87%). ^{1}H NMR ($CDCl_3$): δ 1.15 (m, 24H, CH_2CH_3), 2.00 (two overlapping dq, 16 H, CH_2CH_3), 2.27 (qn, 4H, PCH_2P, J_{PH} = 5.9). ^{31}P{^{1}H} NMR ($CDCl_3$): δ 10.4 (s). UV−vis ($CHCl_3$): 246 (11.0), 320 (12.3), 380 sh (2.30). Anal. Calcd for $C_{18}H_{44}Cl_4P_4Pd_2$: C, 29.25; H, 6.00. Found: C, 29.25; H, 6.06. Recrystallization of **4a** from $CHCl_3$ provided yellow crystals suitable for X-ray diffraction.

***trans*-$Pd_2Br_4(P{-}P)_2$ (P−P = dmpm (3b), depm (4b)).** To a solution of **1b** (0.030 g, 0.038 mmol) in CH_2Cl_2 (10 mL) was added Br_2 (2.2 μL, 0.007 g, 0.044 mmol). The orange-yellow solution rapidly turned yellow. After the solution was stirred for 30 min, the volume was reduced to ~5 mL, and Et_2O (15 mL) was added to precipitate an orange solid. The product was isolated, washed with Et_2O (2 × 10 mL), and dried in vacuo. Yield of **3b**: 0.024 g (78%). ^{1}H NMR ($CDCl_3$): δ 1.82 (br s, 24H, CH_3), 2.70 (qn, 4H, CH_2, J_{PH} = 4.7). ^{31}P{^{1}H} NMR ($CDCl_3$): δ −12.1 (s). UV−vis ($CHCl_3$): 344 (10.5), 404 sh (3.10). Raman, ν(Pd−Br) region: 187 (s), 227 (m), 274 (w), 338 (m). Anal. Calcd for $C_{10}H_{28}Br_4P_4Pd_2$: C, 14.93; H, 3.51. Found: C, 15.23; H, 3.60. Orange prisms of **3b** were formed upon partial evaporation of a $CHCl_3$ solution.

Similarly, a solution of **2b** (0.055 g, 0.072 mmol) in CH_2Cl_2 (10 mL) reacts with Br_2 (3.8 μL, 0.012 g, 0.072 mmol) to yield **4b**. Yield: 0.054 g (82%). ^{1}H NMR ($CDCl_3$): δ 1.11 (m, 24H, CH_2CH_3), 2.13 (unresolved dq, 8H, CH_2CH_3), 2.48 (unresolved dq, 8H, CH_2CH_3), 2.55 (qn, 4H, PCH_2P, J_{PH} = 4.5). ^{31}P{^{1}H} NMR ($CDCl_3$): δ 7.0 (s). UV−vis ($CHCl_3$): 350 (12.3), 406 sh (3.5). Anal. Calcd for $C_{18}H_{44}Br_4P_4Pd_2$: C, 23.58; H, 4.84. Found: C, 23.65; H, 4.86.

$Pd_2I_2(\mu\text{-}I)_2(P{-}P)_2$ (P−P = dmpm (5), depm (6)). To a solution of **1c** (0.061 g, 0.082 mmol) in CH_2Cl_2 (10 mL) was added I_2 (0.025 g, 0.099 mmol). The purple solution containing **5** was stirred for 30 min prior to removal of the solvents by evaporation. The residue was extracted with CH_2Cl_2 (20 mL), the solution filtered and the volume reduced to ~3 mL. A purple solid, precipitated by addition of hexanes (15 mL), was collected, washed with hexanes (2 × 10 mL), and dried in vacuo. Yield: 0.061 g (75%). ^{1}H NMR ($CDCl_3$): δ 2.23 (s, 24H, CH_3), 3.42 (qn, 4H, CH_2, J_{PH} = 4.4). ^{31}P{^{1}H} NMR ($CDCl_3$): δ −19.6 (s). UV−vis ($CHCl_3$): 320 (12.6), 378 (13.1), 534 (6.30), 622 (3.00). IR (CsI pellet): 936 (s), 1358 (s). Λ_M (CH_2Cl_2): 17 Ω^{-1} mol^{-1} cm^2. Anal. Calcd for $C_{10}H_{28}I_4P_4$-

Pd_2: C, 12.10; H, 2.84. Found: C, 12.17; H, 2.76. Large purple block crystals of **5** were isolated from concentrated $CHCl_3$ solutions.

Similarly, a solution of **2c** (0.060 g, 0.070 mmol) reacts with I_2 (0.025 g, 0.099 mmol) to yield **6**. Yield: 0.062 g (80%). ^{1}H NMR ($CDCl_3$): δ 1.22 (m, 24H, CH_2CH_3), 2.45 (br dq, 8H, CH_2CH_3), 2.63 (unresolved dq, 8H, CH_2CH_3), 3.39 (qn, 4H, PCH_2P, J_{PH} = 4.0). ^{31}P{^{1}H} NMR ($CDCl_3$): δ 4.2 (s). UV−vis ($CHCl_3$): 264 (31.4), 320 sh (10.3), 386 (9.70), 546 (4.80), 628 (2.80). Anal. Calcd for $C_{18}H_{44}I_4P_4Pd_2$: C, 19.57; H, 4.01. Found: C, 19.40; H, 4.02.

Acknowledgment. We thank the Natural Sciences and Engineering Council of Canada for funding.

Note Added after ASAP: The version of this article posted ASAP on May 31, 2003, contained an incomplete caption for Figure 8. The correct caption for Figure 8 appears in the version posted on June 3, 2003.

Supporting Information Available: X-ray crystallographic data for the structures of compounds **3a**·2$CHCl_3$, **3b**, **4a**, and **5**. Variable temperature NMR spectra of $Pd_2Cl_2(depm)_2$ (**2a**) (Figure S1). This material is available free of charge via the Internet at http://pubs.acs.org.

IC030048O